The Scientific Temper (2024) Vol. 15 (1): 1726-1732
E-ISSN: 2231-6396, ISSN: 0976-8653
Doi: 10.58414/SCIENTIFICTEMPER.2024.15.1.21
https://scientifictemper.com/

RESEARCH ARTICLE

Three-phase-lags thermoelastic infinite medium model with a spherical cavity *via* memory-dependent derivatives

Nitin Chandel[1*], Lalsingh Khalsa[1], Sunil Prayagi[2], Vinod Varghese[1]

Abstract

The present study examines the impact of a three-phase lags thermoelastic infinite medium with a spherical cavity subjected to thermal shock in the temperature of its internal boundary. In this study, a new time-fractional three-phase-lag thermoelasticity model with memory-dependent derivatives is utilized. From the suggested model, we recover certain previous thermoelasticity models as special instances. Laplace transform techniques are used. The solution to the problem in the transformed domain is obtained by using the Gaver-Stehfest algorithm. The validity of the proposed theory is evaluated through a comparison with the existing literature. The numerical computations are conducted and represented graphically. The numerical values of field variables show significant differences for a specific material, highlighting important points related to the prediction of the new model. The article's physical viewpoints could be helpful in the development of novel materials.

Keywords: Thermoelastic; three-phase-lags; memory-dependent derivative; fractional calculus; spherical cavity; non-simple.

Introduction

The classical uncoupled thermoelasticity model has two issues that do not align with observed physical phenomena: the equilibrium state of heat conduction does not impose constraints on elastic terms, and the heat conduction equation produces an unlimited speed of propagation for thermal waves.

Biot (1956) formulated the theory of coupled thermoelasticity (CTE), which integrates governing equations and resolves the initial dilemma of the classical theory. However, the second paradox, with the coupled theory's heat conduction equation being a parabolic type, was still as is. Lord and Shulman (1967) formulated a novel law of heat conduction, which is classified as hyperbolic and predicts finite propagation speeds for both thermal and mechanical waves. Miller (1971) proposed a limit on a class of constitutive equations, imposing an entropy inequality. Green and Laws (1972), Green and Lindsay (1972), and Suhubi (1975) expanded upon this imbalance. Youssef (2005); Youssef (2005) successfully addressed challenges about generalized thermo-elasticity for an in- finite material with a spherical cavity. Tzou (2014) introduced a dual-phase-lag (DPL) model to study microstructural interactions within solid heat conductors at a microscopic scale, incorporating delay time translation of heat flux vector and temperature gradient. Youssef (2016) successfully solved the initial mathematical model of thermoelasticity with fractional order strain for a homogeneous isotropic one-dimensional thermoelastic half-space, utilizing various thermo-elasticity models.

The present study presents a theoretical framework based on a two-temperature, three-phase lag (TPL) thermoelastic model to elucidate the influence of heat propagation within an infinite medium featuring a spherical cavity. To tackle the challenge of infinite speed propagation, the Fourier model has been modified through the incorporation of a specific time constant, referred to as the phase lag of the heat flux, temperature gradient, and displacement gradient. The closed-form solutions of temperature distribution components across the proposed model are derived using the integral transform approach. The Gaver-Stehfest procedure is employed to derive the numerical Laplace inversion.

[1]Department of Mathematics, M.G. College, Armori, Gadchiroli, India.

[2]Department of Mechanical Engineering, Yeshwantrao Chavan College of Engineering Nagpur

***Corresponding Author:** Nitin Chandel, Department of Mathematics, M.G. College, Armori, Gadchiroli, India, E-Mail: nitinsinghchandel9@gmail.com

How to cite this article: Chandel, N., Khalsa, L., Prayagi, S., Varghese, V. (2024). Three-phase-lags thermoelastic infinite medium model with a spherical cavity *via* memory-dependent derivatives. The Scientific Temper, **15**(1):1726-1732.

Doi: 10.58414/SCIENTIFICTEMPER.2024.15.1.21

Source of support: Nil

Conflict of interest: None.

Received: 08/01/2024 **Accepted:** 10/02/2024 **Published** : 15/03/2024

Mathematical modeling

Notations

q	heat conduction vector	b	discrepancy factor
T	thermodynamic temperature	u	displacement
Φ	conductive temperature	$H(t)$	Heaviside function
k	thermal conductivity	Γ	Gamma function
Q	Internal heat source	ρ	density
e	dilation	s	Laplace parameter
e_{ij}	strain components	δ_{ij}	Kronecker's delta
C_e	specific heat	∇^2	Laplacian operator
τ_i	phase lags $(i=T,q,u)$	t	time
λ,μ	Lame's constants	γ	$(3\lambda+2\mu)\alpha_t$

Modified governing equation

Green and Naghdi (1992) proposed a heat conduction law

$$\vec{q}(P,t+\tau_q)=-k\vec{\nabla}T(P,t+\tau_T) \tag{1}$$

Green and Naghdi (1993) further modeled a heat conduction law

$$\vec{q}(P,t+\tau_q)=-k\vec{\nabla}T(P,t+\tau_T)-k^*\vec{\nabla}u(P,t+\tau_g) \tag{2}$$

where $\partial u/\partial t=T$ and $k^*(>0)$ is a material constant characteristic of the theory.

Chen and Gurtin (1968) proposed two-temperature concepts as

$$\Phi=[1-b(\partial/\partial t)]T\,,\ b>0;\nabla^2=\partial/\partial t \tag{3}$$

Thus, a non-simple non-Fourier law can be proposed using Eqs. (2) and (3)

$$\vec{q}(P,t+\tau_q)=-k[1-b(\partial/\partial t)]\vec{\nabla}T(P,t+\tau_T)-k^*\vec{\nabla}u(P,t+\tau_u) \tag{4}$$

The TPL model by Roy Choudhuri in a modified form:

$$\vec{q}(P,t+\tau_q)=-\,k\vec{\nabla}T(P,t+\tau_T)-k^*\vec{\nabla}u(P,t+\tau_u) \tag{5}$$

and then Eq. (5) was taken with Taylor's expansion as proposed by Jumarie (2010)

$$\vec{q}+\tau_q\frac{\partial\vec{q}}{\partial t}=-\left(\tau_u^*+k\tau_T\frac{\partial}{\partial t}\right)\vec{\nabla}T-k^*\vec{\nabla}u \tag{6}$$

The second order in Taylor's expansion, as expressed in Eq. (2), one obtains

$$\left(1+\tau_q\frac{\partial}{\partial t}+\frac{1}{2}\tau_q^2\frac{\partial^2}{\partial t^2}\right)\vec{q}=-k\left(1+b\frac{\partial}{\partial t}\right)\left(\tau_u^*+k\tau_T\frac{\partial}{\partial t}\right)\vec{\nabla}T-k^*\vec{\nabla}u \tag{7}$$

where $\tau_u^*=k+k^*\tau_u$ and $0\le\tau_u\le\tau_T\le\tau_q$.

The rise in entropy S leads to the energy equation taken by Biot (1956) as

$$\rho C_e\frac{\partial\theta}{\partial t}+\gamma T_0\frac{\partial(\vec{\nabla}\cdot u)}{\partial t}=-\vec{\nabla}\cdot q+Q \tag{8}$$

Taking divergence on both sides of Eq. (8), and using Eq. (9), and differentiating both equations with respect to time, one obtains

$$\left(1+\tau_q\frac{\partial}{\partial t}+\frac{1}{2}\tau_q^2\frac{\partial^2}{\partial t^2}\right)\left(\rho C_e\frac{\partial^2 T}{\partial t^2}+\gamma T_0\frac{\partial^2(\vec{\nabla}\cdot u)}{\partial t^2}-\dot{Q}\right)=k\left(1+b\frac{\partial}{\partial t}\right)\left(\tau_u^*+k\tau_T\frac{\partial}{\partial t}\right)\vec{\nabla}^2\dot{T}-k^*\vec{\nabla}^2T \tag{9}$$

Caputo's fractional-order derivative can be expressed as Caputo and Mainardi (1971).

$$D_a^\alpha Y(t)=\int_a^t\frac{(t-\tau)^{n-\alpha-1}}{\Gamma(n-\alpha)}D^nY(\tau)\,d\tau,\ n-1\le\alpha\le n \tag{10}$$

where the operator D^n denotes n-th derivative operation.

Diethelm (2010) introduced a kernel in the integrand form to enhance the fractional derivative of the Caputo type as follows:

$$D_a^\alpha Y(t)=\int_a^t K_\alpha(t-\xi)Y^{(m)}(\xi)\,d\xi \tag{11}$$

The order derivative, denoted by $Y^{(m)}$, is the kernel function with the following form:

$$K_\alpha(t-\xi)=\frac{(t-\xi)^{m-\alpha-1}}{\Gamma(n-\alpha)} \tag{12}$$

Wang and Li (2011) defined the MDD, introducing the "memory-dependent derivative" to illustrate memory influence. They applied an integral definition of a first-order common derivative of MDD for functions over a sliding interval.

$$D_\tau Y(t)=\frac{1}{\tau}\int_{t-\tau}^t K_\alpha(t-\xi)Y'(\xi)\,d\xi \tag{13}$$

In a particular instance where the kernel $K_\alpha=1$, we find that

$$D_\tau Y(t)=\frac{1}{\tau}\int_{t-\tau}^t Y'(\xi)\,d\xi=\frac{Y(t)-Y(t-\tau)}{\tau}\to\frac{dY}{dt}=Y'(t)=DY \tag{14}$$

If $Y(t)$ and kernel $K_m(t-\xi)$ are differentiable m times around t and ξ, where $m\in$ □ and □ are natural numbers, then

$$D_\tau^m Y(t)=\frac{1}{\tau}\int_a^t K_m(t-\xi)Y^{(m)}(\xi)\,d\xi \tag{15}$$

The equation through the relation between MDD of first and second-order as

$$D_\tau^2 Y(t)=DD_\tau Y(t)=\frac{d}{dt}\left[D_\tau f(t)\right] \tag{16}$$

The m — order MDD moreover fulfills the subsequent relation for any $m\in$ □

$$D_\tau^m Y(t)=D^{m-1}D_\tau Y(t)=\frac{d^{m-1}}{dt^{m-1}}\left[D_\tau Y(t)\right] \tag{17}$$

The MDD equations are practical and can be expressed as a recognized derivative of order, making them useful for real-world problems, as explained in Eq. (12) as

$$\left(D_{\tau_q}^0+\tau_q D_{\tau_q}^1+\frac{1}{2}\tau_q^2 D_{\tau_q}^2\right)\left(\rho C_e\frac{\partial^2 T}{\partial t^2}+\gamma T_0\frac{\partial^2 e}{\partial t^2}-\dot{Q}\right)=\left[k\frac{\partial}{\partial t}\left(1+b\frac{\partial}{\partial t}\right)\left(\tau_u^*+k\tau_T D_{\tau_T}^1\right)+k^*\right]\nabla^2 T \tag{18}$$

Here, Eq. (18) with $b=0$, $T=\Phi$ is reduced to different theories of thermoelasticity:

- Roy Choudhuri (2007) TPL model: $\tau_q \neq 0, \tau_T \neq 0, \tau_u \neq 0$
- Tzou (2014) DPL model: $\tau_q \neq 0, \tau_T \neq 0, \tau_u = 0, k^* = 0$
- Green and Naghdi (1993) GN-III model: $\tau_q = 0, \tau_T = 0, \tau_u = 0$
- Lord and Shulman (1967) LS model: $\tau_q{}^2 = 0, \tau_T = 0, \tau_u = 0, \tau_q = \tau_0 > 0, k^* = 0$
- Biot (1956) CTE model: $\tau_q{}^2 = \tau_T = \tau_u = 0, \tau_q = \tau_0 = 0, k^* = 0$

Eq. (18) with $b \neq 0$, $T \neq \Phi$ is reduced to thermoelasticity theory as given below:

- Mukhopadhyay *et al.* (2011) (MTE) model: $\tau_q{}^2 = \tau_q = \tau_T = \tau_u = 0, k^* = 0$
- Youssef (2006)(YTE) model: $\tau_q{}^2 = \tau_T = \tau_u = 0, \tau_q = \tau_0 > 0, k^* = 0$

Statement of Problem

Let us consider an infinite isotropic medium with a spherical cavity and no external body forces. It is assumed that the spherical cavity occupies the space $D \subset \mathbb{R}^3$ defined by $D = \{(r,\theta,\varphi) \subset \mathbb{R}^3 \mid \ 0 < r \leq a, 0 < \theta \leq 2\pi, 0 < \varphi \leq \pi\}$. The center of the cavity is taken to be the origin of the spherical polar system (r,θ,ϕ), as shown in Figure 1.

Governing equation of thermoelasticity

The governing equations for motion in the absence of body forces

$$\frac{\partial \sigma_{rr}}{\partial r} + \frac{2(\sigma_{rr} - \sigma_{\theta\theta})}{r} = \rho \frac{\partial^2 u}{\partial t^2} \tag{19}$$

The non-zero strain components in terms of displacement are

$$e_{rr} = \frac{\partial u}{\partial r}, e_{\theta\theta} = e_{\phi\phi} = \frac{u}{r}, \sigma_{\theta\theta} = \sigma_{\phi\phi} \tag{20}$$

Then, the stress components are obtained as

$$\sigma_{rr} = \lambda e + 2\mu e_r - \alpha_t (3\lambda + 2\mu) T \tag{21}$$

$$\sigma_{\theta\theta} = \lambda e + 2\mu e_\theta - \alpha_t (3\lambda + 2\mu) T \tag{22}$$

From Eqs. (19)-(22), the equation of motion without external body forces is given by

$$(\lambda + 2\mu)\left(\frac{\partial^2 u}{\partial r^2} + 2\frac{\partial u}{\partial r} - 2\frac{u}{r^2}\right) = \rho \frac{\partial^2 u}{\partial t^2} + \gamma \frac{\partial T}{\partial r} \tag{23}$$

Dimensionless parameter

Let us now present the following non-dimensional variable for convenience:

$$(\hat{r},\hat{u}) = c_0 \eta (r,u),\ (\hat{t},\hat{\tau}_q,\hat{\tau}_T,\hat{\tau}_\upsilon) = c^2{}_0 \eta (t,\tau_q,\tau_T,\tau_\upsilon),$$
$$\hat{T} = \frac{\gamma T}{\lambda + 2\mu}, \hat{\sigma}_{rr} = \frac{\sigma_{rr}}{\lambda + 2\mu}, \eta = \frac{\rho C_e}{\kappa}, c_0 = \sqrt{\frac{\lambda + 2\mu}{\rho}} \tag{24}$$

The form of Eqs. (18), and (19)-(23) are reduced by using Eq. (24) as a non-dimensional quantity and dropping the overhat prime for further calculation

$$\left(D^0_{\tau_q} + \tau_q D^1_{\tau_q} + \frac{1}{2}\tau_q^2 D^2_{\tau_q}\right)\left(\rho C_e \frac{\partial^2 T}{\partial t^2} + p_2 \gamma T_0 \frac{\partial^2 e}{\partial t^2} - p_1 \dot{Q}\right)$$
$$= k\frac{\partial}{\partial t}\left(1 + b\frac{\partial}{\partial t}\right)\left(\tau_u^* + k\frac{\tau_T}{c_0^2 \eta} D^1_{\tau_T}\right)\nabla^2 T + k^* \nabla^2 T \tag{25}$$

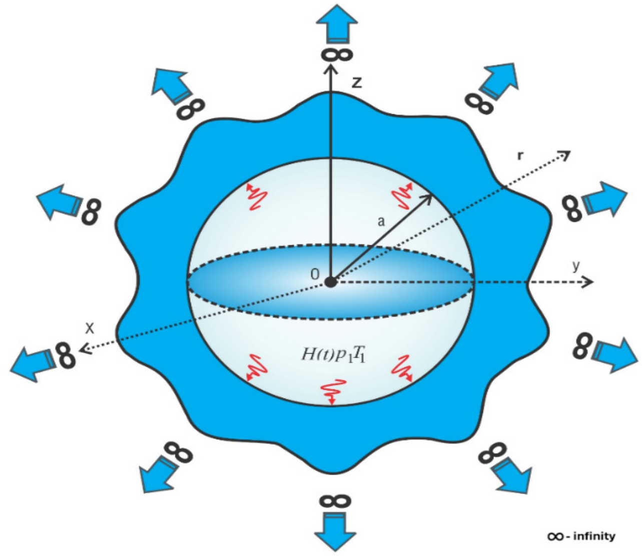

Figure 1: Schematic of the infinite body with a spherical cavity

subjected to initial and boundary conditions

$$T(r,0) = \frac{\partial}{\partial t} T(r,0) = 0 \tag{26}$$

$$T(a,t) = H(t) p_1 T_1 \tag{27}$$

Applying the operator $(1/r^2)\partial/\partial r(r^2)$ in Eq. (23), one gets

$$\nabla^2 e - \nabla^2 T = \frac{1}{c_0^2}\frac{\partial^2 e}{\partial t^2} \tag{28}$$

The stress components of Eq. (21) and (22) are

$$\sigma_{rr} = (1 - \Omega^2) e + \Omega^2 \frac{\partial u}{\partial r} - T \tag{29}$$

$$\sigma_{\theta\theta} = (1 - \Omega^2) e + \Omega^2 \frac{u}{r} - T \tag{30}$$

The resulting in traction-free conditions

$$\sigma_{rr}(a,t) = 0 \tag{31}$$

and the quiescent state

$$\sigma_{rr}(r,0) = \frac{\partial}{\partial t}\sigma_{rr}(r,0) = 0 \tag{32}$$

$$u(r,0) = \frac{\partial}{\partial t} u(r,0) = 0 \tag{33}$$

where

$$\Omega^2 = \frac{\mu}{\lambda + 2\mu}, p_1 = \frac{\gamma}{\lambda + 2\mu}, p_2 = c_0^2 \eta \tau_u^*,\ p^* = k^* \frac{c_0 \gamma}{\lambda + 2\mu} \tag{34}$$

and the cubic dilation e is given by

$$e = \nabla \cdot u = \frac{1}{r^2}\frac{\partial (r^2 u)}{\partial r} = \frac{\partial u}{\partial r} + \frac{2u}{r} \tag{35}$$

Solution of the problem

The Laplace transform is defined by

$$\overline{f}(r,s) = \mathcal{L}[f(r,t)] = \int_0^\infty e^{-st} f(r,t) dt, \mathrm{Re}(s) > 0 \tag{36}$$

By utilizing the convolution theorem, it becomes possible to employ the Laplace transform to the higher-order memory-derivative $D^p_{\tau_i}$, satisfying the property

$$\mathcal{L}[\tau_i D^p_{\tau_i} f(r,t)] = \mathcal{L}[\int_{t-\tau_i}^t K(t-\xi) f^p(r,\xi) d\xi] = s^{p-1} G(s,\tau_i) \mathcal{L}[f(r,t)] \tag{37}$$

and we define the kernel function as

$$K(t-\xi)=1-\frac{2f}{\tau}(t-\xi)+\frac{e^2}{\tau^2}(t-\xi)^p=\begin{cases}1, & \text{if } e=f=0,\ p=0\\ 1-\dfrac{t-\xi}{\tau_i}, & \text{if } e=0,\ f=\dfrac{1}{2},\ p=0\\ \left(1-\dfrac{(t-\xi)}{\tau}\right)^2, & \text{if } e=1,\ f=1,\ p=1\end{cases} \quad (38)$$

where is the delay time τ ; e and f are constants, and $p\in\mathbb{R}$, respectively.

Taking Laplace Transform as written by Debnath and Bhatta (2006) on Eqs. (25) and (28)-(33), one get

$$(\nabla^2-l_2)\overline{T}=l_3(\gamma T_0 s\overline{e}-\overline{Q}) \quad (39)$$

$$[\nabla^2-(1/c_0^2)s^2]\overline{e}=\nabla^2\overline{T} \quad (40)$$

$$\overline{\sigma}_{rr}=(1-\Omega^2)\overline{e}+\Omega^2\frac{\partial\overline{u}}{\partial r}-\overline{T} \quad (41)$$

$$\overline{\sigma}_{\theta\theta}=\overline{\sigma}_{\phi\phi}=(1-\Omega^2)\overline{e}+\Omega^2\frac{\overline{u}}{r}-\overline{T} \quad (42)$$

where

$$\begin{aligned}&l_0=ks(1+bs)[p_2+k(\tau_T/c_0^2\eta)G(s,\tau_T)]+k^*,\\&l_1=[1+G(s,\tau_q)+(1/2)s\,G(s,\tau_q)]/l_0,\\&l_2=l_1(\rho C_e s^2),\ l_3=l_1p_1s,\\&G(s,\tau_i)=(1-e^{-s\tau_i})\left(1-\frac{2f}{s\tau_i}+\frac{2e^2}{s^2\tau_i^2}\right)-\left(e^2-2f+\frac{2e^2}{s\tau_i}\right)e^{-s\tau_i}\end{aligned} \quad (43)$$

Now $\overline{e}$ eliminating from Eqs. (39) and (40), one gets

$$(\nabla^4-A_1\nabla^2+A_2)\overline{T}=l_3(l_4-\nabla^2)\overline{Q} \quad (44)$$

where

$$A_1=l_2+l_3\gamma T_0 s+l_4,\ A_2=l_2l_4,\ l_4=s^2/c_0^2 \quad (45)$$

Since A_1 and A_2 are real positive numbers, then Eq.(44) becomes

$$(\nabla^2-m_1^2)(\nabla^2-m_2^2)\overline{T}=l_3(l_4-\nabla^2)\overline{Q} \quad (46)$$

where m_1^2 and m_2^2 are the roots of the characteristics equation

$$m^4-A_1m^2+A_2=0 \quad (47)$$

Henceforth, we consider internal heat sources as

$$Q(r,t)=q_0H(t)\delta(r)/r \quad (48)$$

Therefore Eq.(46) become

$$(\nabla^2-m_1^2)(\nabla^2-m_2^2)\overline{T}=\frac{q_0l_3}{s}(l_4-\nabla^2)\frac{\delta(r)}{r} \quad (49)$$

Use the Hankel transformation

$$H_{0\zeta}[\overline{f}(r,s)]=\hat{\overline{f}}(\zeta,s)=\int_0^a rJ_0(\zeta r)\overline{f}(r,s)dr \quad (50)$$

and inversion of Hankel transformation is

$$\overline{f}(r,s)=\int_0^\infty \hat{\overline{f}}(\zeta,s)\xi J_0(\zeta r)dr \quad (51)$$

where $J_0(\zeta r)$ is the Bessel function of the first kind of order 0, and $J_0(\zeta a)=0$.

The Hankel transformation on Eq. (49) has been applied, resulting as

$$(\zeta^2+m_1^2)(\zeta^2+m_2^2)\overline{T}=q_0l_3l_4/s \quad (52)$$

Then the solution of the function $\overline{T}(r,s)$ in Laplace domain is

$$\overline{T}(r,s)=\frac{q_0l_3l_4}{s(m_1^2-m_2^2)}\left[K_0(m_2r)-K_0(m_1r)\right] \quad (53)$$

where $K_0(m_ir),\ i=1,2$ is the second kind of modified Bessel function of zero order, and we have $(d/dr)K_0(m_ir)=-m_iK_1(m_ir)$ and $\nabla^2(K_0(m_ir))=m_i^2K_0(m_ir)$.

Substituting equation (53) into $u=\partial\overline{T}/\partial r$, one obtains

$$u=\frac{q_0l_3l_4}{s(m_1^2-m_2^2)}\left[m_1K_1(m_1r)-m_2K_1(m_2r)\right] \quad (54)$$

where $K_1(m_ir),\ i=1,2$ is the second kind of modified Bessel function of one order.

The cubic dilation e can be obtained using Eq. (54) as

$$e=\frac{q_0l_3l_4}{rs(m_1^2-m_2^2)}\left[m_1\left(K_1(m_1r)-rK_0(m_1r)\right)+m_2\left(rK_0(m_2r)-K_1(m_2r)\right)\right] \quad (55)$$

Substituting Equations (53)-(55) in Equations (41)-(42), one obtains

$$\overline{\sigma}_{rr}=\frac{q_0l_3l_4}{rs(m_1^2-m_2^2)}\begin{bmatrix}(1-2\Omega^2)[m_1K_1(m_1r)-m_2K_1(m_2r)]-\\(m_1-1)rK_0(m_1r)+(m_2-1)rK_0(m_2r)\end{bmatrix} \quad (56)$$

$$\overline{\sigma}_{\theta\theta}=\frac{q_0l_3l_4}{rs(m_1^2-m_2^2)}\begin{bmatrix}[(1-\Omega^2)m_2-1]rK_0(m_2r)-[(1-\Omega^2)m_1-1]\\\times rK_0(m_1r)+m_1K_1(m_1r)-m_2K_1(m_2r)\end{bmatrix} \quad (57)$$

The Gaver-Stehfest algorithm as proposed by Stehfest (1970) is used to solve a problem in the Laplace transform domain, obtaining conductive temperature increment, dynamical temperature increment, displacement, and stress distributions in the time domain

$$\begin{aligned}&f(t)\approx f_n(t)=\frac{\mathrm{In}(2)}{t}\sum_{n=1}^{L}(-1)^{n+L/2}a_n\,F\left[\frac{n\mathrm{In}(2)}{t}\right],\\&a_n=\sum_{k=[(n+1)/2]}^{\min(n,L/2)}\frac{k^{L/2}(2k)!}{(L/2-k)!k!(k-1)!(n-k)!(2k-n)!}\end{aligned} \quad (58)$$

where $F[.]$ is the Laplace transform of $f(t)$, $n\geq 1,\ t>0,$ $1\leq L\leq n$.

Numerical results and their discussion in the time domain

The numerical illustration illustrates the use of hypothetical copper-like as a thermoelastic material to achieve the desired objective, considering various physical constant values Youssef (2005), for which $k=386$ kg m k^{-1}s^{-3}, $\alpha_t=1.78\times10^{-5}$ k^{-1}, $\rho=8954$ kg m^{-3}, $T_0=293$ K, $C_e=383.1$ m^2 k^{-1} s^{-2}, $\lambda=7.76\times10^{10}$ kg m^{-1} s^{-2}, $\mu=3.86\times10^{10}$ kg m^{-1} s^{-2}. In our numerical calculations, we take $\tau_q=0.03$ s, $\tau_T=0.03$ s, $\tau_\upsilon=0.05$ s, $k=7$. It is well stated in the article of Mondal and Kanoria (2019), which aligns with the stability requirement stated in Quintanilla and Racke (2008); under three-phase lag heat conduction occurs, the solutions are always exponentially stable, if $k^*\tau_q<\tau_\upsilon^*<2k^*\tau_T/\tau_q$.

Model Validation

The present model undergoes a comparison analysis with many models in order to evaluate its reliability, as illustrated in Figure 2. When the first kernel function of Eq. (38) is

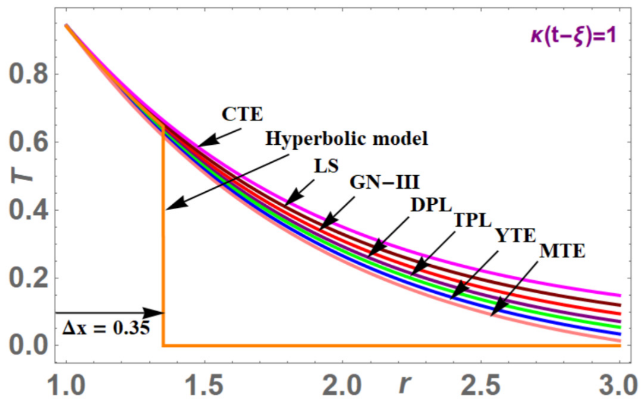

Figure 2: Comparisons between the different theories of *thermoelasticity*

assumed to be 1, it is possible to estimate the differential over time up to the limit of D_{τ_i}, as the hysteresis factor τ_i approaches zero.

According to theoretical considerations, it is projected that when the hysteresis factor is low, the MDD will undergo a transition into a triple/dual-phase hysteresis model. The model we have proposed, which incorporates complex differential partial equations, can be simplified to a parabolic model when uniform initial conditions $\tau_q = \tau_T = 0$ are applied. In this simplified model, the temperature discrepancy factor $b = 0$, $k^* = 0$ and considering two temperatures as $\theta = \Phi$ in Eqs. (25), are considered. This simplifies the model to the coupled classical thermoelasticity (CTE) model . In the present context, when η is set to zero, the model transforms a coupled hyperbolic model to an uncoupled hyperbolic model. When $\tau_u^* = 0$ is taken into account, the current model will shift from a coupled hyperbolic model to an uncoupled one. Based on Xu and Wang (2018), the heat propagation velocity can be determined as $V = \{1/[\tau_q D_q + (1/2)\tau_q^2 D_q^2]\}^{1/2}$ using Eq. (25). Given that the kernel function in Eq. (38) is equal to 1, the result obtained by taking $\tau_q = 0.04$ and $\tau_q^2 = 0.0016$ is $V = \{50\}^{1/2}$. The dimensionless propagation distance, denoted as $\Delta x = Vt = \{50\}^{1/2} t = 0.35$ (here $t = 0.05$), exhibits a strong concurrence with the numerical forecast, as depicted in Figure 2. The integral across a region represents the heat absorbed from an external heat source. In contrast, the temperature distributions of distinct models show distinct heat transfer mechanisms occurring at a particular moment. The figure clearly illustrates that all models exhibit distinct variations in values in close proximity to surface boundaries, and this variation diminishes as the distance and sectional heat supply increase. The temperature profile reaches its peak values in close proximity to the inner curved surface and subsequently diminishes until it reaches zero.

Effect of kernel function response along the radius

The RED line refers to the kernel function $\kappa(t-\xi) = 1$; the BLUE line refers to the kernel function $\kappa(t-\xi) = 1-(t-\xi)/\tau_i$, and the PURPLE line for the kernel function $\kappa(t-\xi) = (1-(t-\xi)/\tau_i)^2$. The temperature distribution exhibits an initial high value at the onset of the curved spherical cavity due to the presence of sectional thermal shock, followed by a progressive stabilization as the parameter *r* approaches infinity, as depicted in Figure 3. The findings of the study indicate a direct proportion to positive phase-lag difference and kernel function values, with the coupled scenario exhibiting higher temperatures than the uncoupled scenario.

Figure 4 shows trends in displacement curves, with initial values, acting with high compressed force due to sectional heat flux accumulation. The uncoupled case also showed a high-magnitude displacement trend as it tends to infinity. According to Figure 5, the radial stress exhibits a monotonically decreasing trend and recovers in the later stage along the radial direction as the kernels vary. Starting from zero values, it reaches the deep trough and gradually increases till it approaches zero. The fall in stress during the first phases and later stages can be attributed to an increase in the rate of heat propagation. This decrease in stress is primarily driven by the compressive force and later taken over by tensile force, which gradually approaches zero as its radius approaches infinity. Figure 6 illustrates that the compressive force significantly reduces the tangential stress

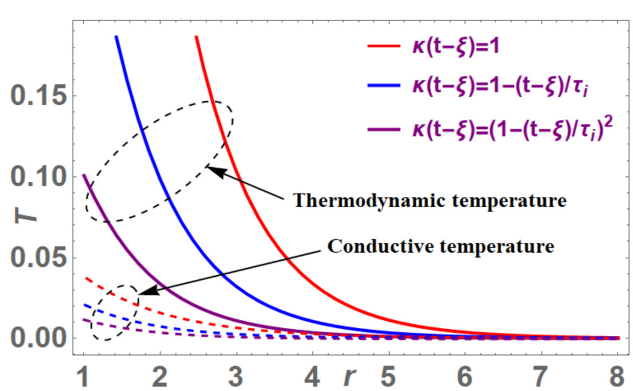

Figure 3: Temperature profile with different kernels along r for fixed t

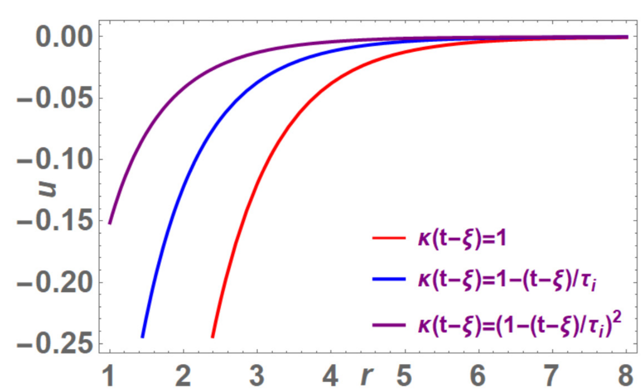

Figure 4: Displacement profile with different kernels along r for fixed t

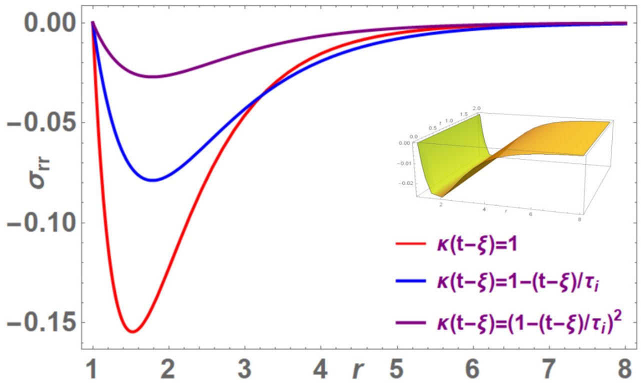

Figure 5: Radial stress with different kernels along r for fixed t

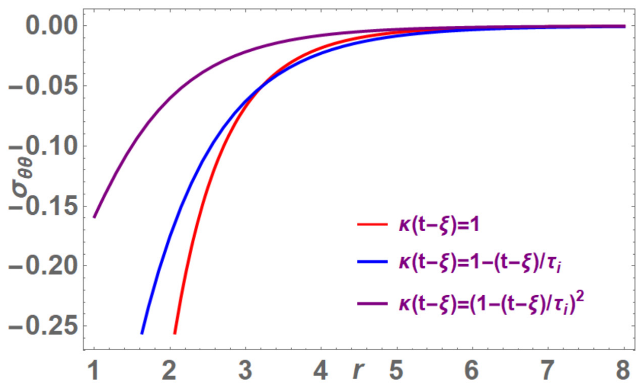

Figure 6: $\sigma_{\theta\theta}$ with different kernels along r for fixed t

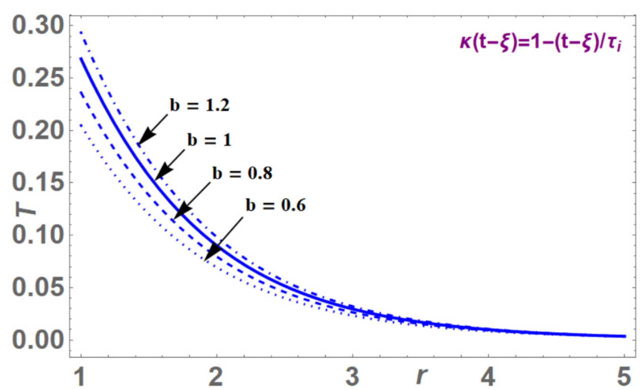

Figure 7: Temperature distribution along r for various b values for fixed kernel

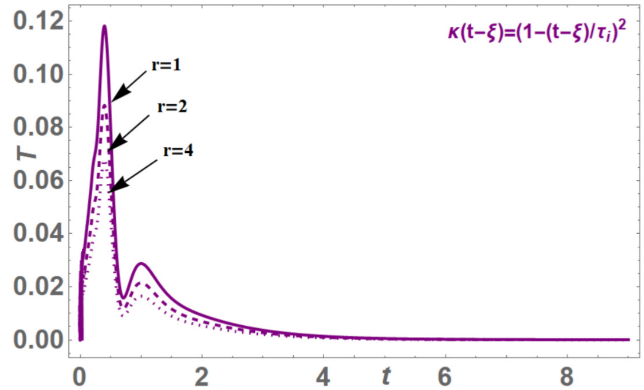

Figure 8: Temperature distribution along t for various r values for fixed kernel

at the start of the curved spherical cavity. As the radius approaches infinity, the strong tensile force steadily raises the tangential stress and eventually stabilizes it at zero.

Effect of temperature discrepancy factor on temperature profile

Figure 7 illustrates a graph showcasing the temperature distribution along r for the kernel $\kappa(t-\xi)=1-(t-\xi)/\tau_i$ at fixed time $t=1.5$. The graph comprises a variety of data points that correspond to distinct values of the temperature discrepancy factor, denoted as *b*. When the value of $b=0$, it indicates that the model mentioned above has been simplified to a theory that considers only one temperature. On the contrary, $b\neq 0$ it signifies the existence of two temperature theories.

The homogeneous dispersion of thermal energy shows that the spherical cavity boundary exhibits the highest temperature. At the value of $b=1.2$, the temperature graph displays a pronounced increase due to the conversion of heat energy into strain energy. The primary cause of this phenomenon is commonly ascribed to the element of high-temperature discrepancy. The observed outcome is consistent with what was reported in a prior publication by Zenkour and Abouelregal (2016).

Histories of thermal coupling over time

This section examines the correlation between temperature and time at various radial points, presenting a graphical representation of their changing patterns in Figure 8 for the kernel function $\kappa(t-\xi)=(1-(t-\xi)/\tau_i)^2$. The temperature response distribution is influenced by heat wave propagation at the curved spherical cavity. It demonstrates a peak in the temperature curve, followed by a gradual decline until a stable state, attributed to heat shock. Variations in peak positions are due to damp-heat wavefront arrival times.

Conclusion

The study develops a comprehensive three-phase-lags thermoelastic infinite medium model with a spherical cavity *via* memory-dependent derivatives, examining heat flow under rapid temperature increase.The numerical results yield several inferences:

- 'Memory-dependent derivatives' non-Fourier effects significantly impact thermal field response history and distribution, with energy dissipation potentially causing temperature decrease without heat transfer.
- A revised categorization system for materials based on memory-dependent derivative parameters evaluates

heat conduction capacity, considering thermoelasticity at two temperatures *via* memory-dependent derivative.

- The phase-lag heat flux and temperature gradient significantly impact thermal field variables in memory-dependent derivatives time.
- The theories of CTE, Hyperbolic model, LS, GN-III, DPL, TPL, YTE, MTE are derived as specific instances and illustrated graphically; it shows a good agreement.

References

Biot, M.A. (1956). Thermoelasticity and irreversible thermodynamics, J. Appl.Phys., Vol. 27, pp.240-253. DOI: 10.1063/1.1722351.

Chen, P. J. and Gurtin, M. E. (1968). On a theory of heat conduction involving two temperatures, Z. Angew. Math. Phys., Vol. 19, pp. 559-577. DOI: 10.1007/BF01594969.

Caputo, M. and Mainardi, F. (1971). Linear models of dissipation in anelastic solids, La Rivista del Nuovo Cimento, Vol. 1, pp. 161-198. DOI: 10.1007/BF02820620.

Diethelm, K. (2010). The analysis of fractional differential equations: an application-oriented ex- position using differential operators of caputo type, SSBM, 2010.

Debnath, L. and Bhatta, D. (2006). Integral Transforms and their Applications, Chapman and Hall/CRC, New York. DOI: 10.1201/9781420010916.

Green, A. E. and Laws, N. (1972). On the entropy production inequality, Arch. Rational Mech.Anal., Vol. 45, pp. 47-53. DOI: 10.1007/BF00253395.

Green, A. E. and Lindsay, K. A. (1972). Thermoelasticity, J. Elast., Vol. 2, pp. 1-7. DOI: 10.1007/BF00045689.

Green, A. E. and Naghdi, P. M. (1992). On undamped heat waves in an elastic solid, J. Therm.Stresses, Vol. 15, no. 2, pp. 253- 264. DOI: 10.1080/01495739208946136.

Green, A. E. and Naghdi, P. M. (1993). Thermoelasticity without energy dissipation, J. Elast., Vol.31, pp. 189-208. DOI: 10.1007/BF00044969.

Jumarie, G. (2010). Derivation and solutions of some fractional Black-Scholes equations in coarse- grained space and time - Application to Merton's optimal portfolio, Comput. Math. Appl., Vol. 59, no. 3, pp. 1142-1164. DOI: 10.1007/BF00044969.

Lord, H. W. and Shulman, Y. (1967). A generalized dynamical theory of thermoelasticity, J. Mech.Phys. Solids, Vol. 15, no. 5, pp. 299-309. DOI: 10.1016/0022-5096(67)90024-5.

Mller, I. (1971). The coldness, a universal function in thermo- elastic solids, Arch. Rat. Mech. Anal., Vol. 41, pp. 319-332. DOI: 10.1007/BF00281870.

Mukhopadhyay, S., Prasad, R. and Kumar R. (2011). On the theory of two-temperature thermoelasticity with two phase-lags, J. Therm. Stress, Vol. 34, no. 4, pp. 352-365. DOI: 10.1080/01495739.2010.550815.

Mondal, S. and Kanoria, M. (2019). Thermoelastic solutions for thermal distributions moving over thin slim rod under memory-dependent three-phase lag magneto-thermoelasticity, Mech. Based Des. Struct. Mach., pp. 1-22. DOI: 10.1080/15397734.2019.1620529.

Quintanilla, R. and Racke, R. (2008). A note on stability in three-phase-lag heat conduction, Int. J. Heat Mass Transf.,Vol.51, 1-2,no.pp.24-9.DOI:10.1016/j.ijheatmasstransfer.2007.04.045

Roy Choudhuri, S. K. (2007). On a thermoelastic three-phase-lag model, J. Therm. Stresses, Vol.30, no. 3, pp. 231-238. DOI: 10.1080/01495730601130919.

Stehfest, H. (1970). Algorithm 368, Numerical inversion of Laplace transforms, Commun. Assn.Comput. Mach., Vol. 13, no. 1, pp. 47-49. DOI: 10.1145/361953.361969.

Suhubi, E. S. (1975). Thermoelastic solids. In: Cemal Eringen, A. (ed.) continuum mechanics of single-substance bodies, Elsevier, Vol. II, pp. 173-265.

Tzou, D. Y. (2014). Macro-to microscale heat transfer: the lagging behavior, John Wiley & Sons, U.S.A.

Wang, J. L. and Li, H. F. (2011). Surpassing the fractional derivative: concept of the Memory dependent derivative, Comput. Math. Appl., Vol. 62, pp. 1562-1567. DOI: 10.1016/j.camwa.2011.04.028.

Xu, G. and Wang, J. (2018). Analytical solution of time-fractional Cattaneo heat equation for finite slab under pulse heat flux, Appl. Math. Mech. -Engl. Ed., Vol. 39, pp. 1465-1476. DOI: 10.1007/s10483-018-2375-8.

Youssef, H. M. (2005). Dependence of modulus of elasticity and thermal conductivity on reference temperature in generalized thermoelasticity for an infinite material with a spherical cavity, Appl. Math. Mech., Vol. 26, pp. 470-475. DOI: 10.1007/BF02465386.

Youssef, H. M. (2005). State-space approach on generalized thermoelasticity for an infinite mate- rial with a spherical cavity and variable thermal conductivity subjected to ramp-type heating, Can. Appl. Math. Q., Vol. 13, pp. 369-390.

Youssef, H. M. (2006). Theory of two-temperature-generalized thermoelasticity, IMA J Appl Math, Vol. 71, no. 3, pp. 383-390. DOI: 10.1093/imamat/hxh101.

Youssef, H. M. (2016). Theory of generalized thermoelasticity with fractional order strain, J. Vib.Control, Vol. 22, no. 18, pp. 3840-3857. DOI: 10.1177/10775463145668.

Zenkour, A. M. and Abouelregal, A. E. (2016). Non-simple magneto- thermoelastic solid cylinder with variable thermal conductivity due to harmonically varying heat, Earthq. Struct., Vol. 10, no. 3, pp. 681-697. DOI: 10.1007/BF00044969.

Appendix A

The kernel function

$$G(s,\tau_i) == \begin{cases} 1-e^{-s\tau_i}; & \kappa(t-\xi)=1 \\ 1-\dfrac{1-e^{-s\tau_i}}{s\tau_i}; & \kappa(t-\xi)=1-\dfrac{t-\xi}{\tau_i} \\ \left(1-\dfrac{2}{s\tau_i}\right)+\dfrac{2(1-e^{-s\tau_i})}{s^2\tau_i^{\,2}}; & \kappa(t-\xi)=\left(1-\dfrac{t-\xi}{\tau_i}\right)^2 \end{cases} \tag{A1}$$